Angelica Sinensis polysaccharide attenuates chondrocyte ferroptosis and alleviates cartilage degeneration in OA

Guangrong Yin
Graduate School of Dalian Medical University
Su Ni
Medical Research Center, The Affiliated Changzhou No.2 People's Hospital of Nanjing Medical University
Liangliang Wang
Department of Orthopedics, The Affiliated Changzhou No.2 People's Hospital of Nanjing Medical University
Nanwei Xu
Department of Orthopedics, The Affiliated Changzhou No.2 People's Hospital of Nanjing Medical University
Gongyin Zhao
Department of Orthopedics, The Affiliated Changzhou No.2 People's Hospital of Nanjing Medical University
Ruixia Zhu
Department of Orthopedics, The Affiliated Changzhou No.2 People's Hospital of Nanjing Medical University
Shijie Jiang
Department of Orthopedics, The Affiliated Changzhou No.2 People's Hospital of Nanjing Medical University
Jiahao Wang
Graduate School of Dalian Medical University
Baojun Zhou
Department of Orthopedics, The Third Affiliated Hospital of Gansu University of Chinese Medicine
Yuji Wang (✉ yujiwang@sohu.com)
Department of Orthopedics, The Affiliated Changzhou No.2 People's Hospital of Nanjing Medical University

---

Research Article

Keywords: ferroptosis, osteoarthritis, angelica sinensis polysaccharide, SLC7A11, Nrf2

Posted Date: May 6th, 2022

DOI: https://doi.org/10.21203/rs.3.rs-1628781/v1

Abstract

Osteoarthritis (OA) is one of the common degenerative diseases. Its main pathogenesis is the progressive destruction of articular cartilage, synovitis, subchondral bone, and periarticular muscle changes. Accumulating evidence demonstrates that ferroptosis may be important in the progression of OA. Angelica Sinensis polysaccharide (ASP), a traditional Chinese medicine, possesses antioxidative, anti-inflammatory and anti-apoptotic properties in chondrocytes. In this study, we observed that ferroptosis participates in OA's progression. Importantly, GPX4, FTH1, and GSH expressions were higher while MDA level was down-regulated in the control group than in the OA group. Chondrocyte ferroptosis induced by erastin or IL-1β was rescued to varying degrees by ASP, Fer-1, or DFO in vitro. The anti-ferroptotic effect of ASP was related to Nrf2 nuclear transfer. In the rat joints, both DFO and ASP alleviated the cartilage damage induced by DMM or erastin. In summary, Chondrocyte ferroptosis plays a key role in OA progression, and ASP can partially rescue chondrocyte ferroptosis through the Nrf2-SLC7A11-GPX4 axis, supporting the view that ASP is an excellent inhibitor of ferroptosis, its inhibition of ferroptosis provides a potential therapeutic target for the treatment of OA.

Significance Statement

We illustrated that chondrocyte ferroptosis was involved in cartilage degeneration during osteoarthritis progression. In addition, we demonstrated that ASP can decrease the expression of MMPs in OA chondrocytes and inhibit the degradation of cartilage ECM. Moreover, ASP significantly elevated SLC7A11 and GPX4 levels and inhibited chondrocyte ferroptosis by promoting Nrf2 nuclear translocation. We believe our observations are important and could help in the development of new drugs to treat OA.

Introduction

The main clinical symptoms of knee osteoarthritis (OA) are alternating and intermittent pain, swelling, and limited movement, ultimately leading to joint deformity (Sharma, 2021). To date, OA has become one of the main diseases compromising people's ability to work and resulting in disability (Toh et al., 2017). In the pathophysiological process of OA, chondrocytes, as the only cells of cartilage species, undergo various forms of programmed death, including apoptosis, necroptosis and pyroptosis (Riegger and Brenner, 2019; An et al., 2020; Jiang et al., 2020). However, the mechanisms of ferroptosis involved in OA have rarely been reported. As a new representative of programmed cell death, ferroptosis may have considerable potential to interfere with OA pathophysiological processes (Yao et al., 2021).

Ferroptosis, a form of programmed cell death, was first reported by Dixon et al. in 2012 (Dixon et al., 2012). Shrunken mitochondria, increased mitochondrial membrane density, decreased or absent mitochondrial cristae, outer mitochondrial membrane rupture, normal nuclear size and a lack of chromatin condensation are cellular morphological characteristics of ferroptosis (Xie et al., 2016). The mechanisms of ferroptosis include iron homeostasis, glutathione depletion, inactivation of the antioxidant enzyme glutathione peroxidase 4 (GPX4), and lipid peroxidation (Stockwell et al., 2017).

Solute carrier family 7 member 11 (SLC7A11) is the catalytic subunit of cystine transporter system Xc-, which takes cystine from the extracellular environment for conversion into cysteine in the cytoplasm by a reduction reaction that consumes NADPH. Cysteine is then used to synthesize glutathione (GSH), which is an effective lipid peroxidation scavenger and an essential cofactor, to promote GPX4 production and thus prevent phospholipid peroxidation and protect cells from ferroptosis (Yang et al., 2014). However, recent studies have suggested that nuclear factor erythroid 2-like 2 (Nrf2), an initiating gene that inhibits ferroptosis, is closely related to SLC7A11 (Qiang et al., 2020). In addition, iron metabolism and glutathione synthesis are also regulated by the Nrf2 signaling pathway (Stockwell et al., 2017; Dodson et al., 2019). Nrf2 is one of the most important transcription factors regulating the antioxidant response. Under nonstress conditions, Nrf2 and Keap1 are combined, whereas under stress conditions, Nrf2 is released into the nucleus, interacts with MAF, and binds to the antioxidative response element (ARE), generating an Nrf2-MAF dimer to promote downstream gene transcription, including NAD(P)H, quinone oxidoreductase 1 (NQO1), glutathione-S- transferases (GSTs), glutamate-cysteine ligase catalytic (GCLC), and hem oxygenase-1 (HMOX1) (Bellezza et al., 2018; Tonelli et al., 2018). Some reports suggest that activation of the Nrf2 pathway in many compounds can prevent toxic or carcinogenic effects; thus, Nrf2 activation is considered a promising cellular protection strategy (Moon and Giaccia, 2015; Menegon et al., 2016).

Angelica Sinensis polysaccharide (ASP) is composed of galactose, arabinose, glucose, xylose, rhamnose, glucuronic acid and fructose (Wang et al., 2003; Sun et al., 2005). Previous reports have shown that ASP plays an important role in antioxidation, antiapoptosis, and immune regulation and alleviates hepatocyte damage (Cao et al., 2018; Gu et al., 2019). Zhuang C et al. reported that ASP has protective effects on chondrocytes, such as autophagy promotion and a reduction in chondrocyte apoptosis induced by H_2O_2 (Zhuang et al., 2020). However, the effects of ASP on ferroptosis in OA remain unclear. In our study, we aimed to explore the effect of ASP on chondrocyte ferroptosis in OA and the associated mechanisms.

Materials And Methods

Reagents

Collagenase II (Worthington Biochemical Corp., Lakewood, NJ, USA) was dissolved in DMEM-F12 at 1.5 mg/ml to digest articular cartilage. Erastin (USA, E-7781) and ferrostain-1 (USA, SML0583) were purchased from Sigma-Aldrich. BODIPY 581/591 C11 (USA, D3861) was purchased from Thermo Fisher. The LDH Cytotoxicity Assay Kit and Cell Counting Kit-8 (CCK-8) were purchased from Beyotime Biotechnology (Shanghai, China). Nrf2 antibody (16396-1-AP), collagen Ⅱ (18165-1-AP) and SLC7A11 antibodies (26864-1-AP) were purchased from Proteintech (Wuhan, China). GPX4 antibody (A11243) and FTH1 antibody (A19544) were purchased from Abcam. ASP was purchased from Shanghai Yilin Biotech. Co., Ltd. (Shanghai, China). ASP had a purity greater than 92% pure, and the average molecular weight was 85.0 kDa.

Subjects

The study was approved by the ethics committee of the Second People's Hospital of Changzhou, Jiangsu, China. Cartilage specimens were collected from the knees of patients with clinical stage III or IV (K-L score) OA when they underwent joint replacement, and tissue was obtained from non-damaged regions and obviously damaged regions of the joints (Fig. 1A). All participants signed an informed consent form before the operation. All participants signed an informed consent form before the operation. Patient information is shown in Supplementary Table 1.

Isolation and Culture of Chondrocytes

All tissues were cut into pieces as finely as possible, partially digested by collagenase II at 1 mg/mL in Dulbecco's modified Eagle's medium DMEM/F12 (Gibco BRL, Grand Island, NY, USA) at 37℃ for 4 hours, and filtered through a 70-μm cell strainer (BD, Durham, NC, USA). Finally, 10% fetal bovine serum, 50 μg/mL ascorbic acid (AA, Sigma), 100 U penicillin and 100 μg/ml streptomycin were added to the DMEM/F12 medium for culture in a standard cell culture chamber containing 5% CO2. Nonadherent cells were removed 2 days later. Adherent cells were split at a ratio of 1:2 until 90% confluence. Passage 2–3 chondrocytes were used in subsequent experiments. The remaining specimens were cryopreserved and then ground with liquid nitrogen and preserved.

Cell Viability Assay

The Cell Counting Kit-8 (CCK-8) was used to detect chondrocyte activity in the experiment. Chondrocytes were cultured in 96-well plates at a density of 5×10^3 cells/well. After 12 hours, the chondrocytes were pretreated with 30 μg/ml ASP for 24 hours. Next, the cells were treated with 5 μM erastin, 5 μM erastin and 30 μg/ml ASP, and 5 μM erastin and 10 μM Fer-1 for 24 hours and 48 hours. After incubation, the cells were washed twice with PBS, and then 100 μl of 10% CCK-8 solution was added to each well, followed by incubation at 37℃ for 1.5 hours. The absorbance at 450 nm-650 nm was detected by an absorbance microplate reader (Epoch Bio-Tek Instruments, USA).

Detection of lipid ROS

Chondrocytes were spread in a 24-well plate at a density of 3×10^4 cells/well. After 24 hours, the chondrocytes were treated with 5 μM erastin, 5 μM erastin and 30 μg/ml ASP, or 5 μM erastin and 10 μM Fer-1 for 24 hours. Lipid ROS levels were measured with the C11 BODIPY fluorescent probe according to the manufacturer's instructions. Briefly, the chondrocytes were cleaned three times with PBS and treated with 5 μM C11 BODIPY for 25 min at 37℃ in the dark. After incubation, the chondrocytes were washed with PBS three times and observed under a fluorescence microscope (Nikon Eclipse Ti, Japan).

Western blot analysis

Chondrocytes were spread on 6-well plates at a density of 4×10^5 cells/well. After 12 hours, the chondrocytes were treated consistently with the above conditions. Then, the chondrocytes were lysed on ice for 15 min with 200 μl RIPA buffer containing 1% proteinase inhibitor cocktail and boiled for 5 min after removal of the medium. The protein concentration was determined by a BCA Protein Assay kit.

Equal amounts of protein were electrophoresed on a 15% SDS–PAGE gel and transferred to a polyvinylidene fluoride (PVDF) membrane. Then, the membranes were blocked with 5% skimmed milk at room temperature for 1 hour and incubated overnight at 4°C with the primary antibody according to the instructions (1:1000 dilution). Then, the membranes were incubated with secondary antibodies at room temperature for 1 hour. Protein bands were detected with SuperSignal West Pico Plus (Thermofisher Scientific, USA) ECL kit, and relative expression levels were quantified using ImageJ software.

Immunofluorescence staining

Chondrocytes were uniformly seeded on a 24-well plate containing slides. After the cells were treated, they were immobilized at room temperature for 15 min with 4% paraformaldehyde. After 20 minutes of 0.5% Triton X-100 permeation at room temperature, 5% BSA was used for blocking for 1 hour. Primary antibodies diluted with 5% BSA (1:200) were incubated at 4°C overnight. After treatment, the slides were washed three times with PBS and incubated with secondary antibody at room temperature for 1 hour in the dark. The slides were washed again with PBS 3 times, the nuclei were counterstained with DAPI for 10 minutes in the dark and then observed under a fluorescence microscope.

Lactate dehydrogenase (LDH) assay

To measure the release of lactate dehydrogenase, chondrocytes were evenly distributed on a 96-well plate at a density of 5×10^3 per well, with 3–6 wells per group. After treatment as described above, LDH levels were determined according to the manufacturer's instructions. In brief, the supernatant of the cells was moved to a new 96-well plate and incubated for 1 hour with LDH reagent. Then, the absorbance at 490 nm was detected by an absorbance microplate reader.

Glutathione (GSH) assay in cartilage tissue

GSH reacts with 5,5'-dithiobis-2-nitrobenoic acid (DTNB) to produce 2-nitro-5-mercaptobenzoic acid (TNB) (yellow) and oxidized glutathione (GSSG). GSH levels were determined according to the manufacturer's instructions for the Reduced Glutathione Assay Kit (BC1175, Solarbio, Beijing, China). Briefly, the specimens were washed with PBS 3 times and frozen. Then, the specimens were ground with liquid nitrogen, mixed with GSH reagent and moved to 96-well plates, and the absorbance was measured at 412 nm.

Malondialdehyde (MDA) assay in cartilage tissue.

MDA can condense with thiobarbituric acid (TBA) and show a brownish-red color under acidic and high-temperature conditions. MDA levels were determined according to the manufacturer's instructions for the Micro Malondialdehyde (MDA) Assay Kit (BC0025, Solarbio). Briefly, the specimens were washed with PBS 3 times and frozen. Then, the specimens were ground with liquid nitrogen, mixed with MDA reagent and moved to 96-well plates, and the absorbance was measured at 532 nm.

Immunohistochemistry

Cartilage tissue was taken from SD rats. The cartilage was sectioned after paraffin embedding, and endogenous peroxidase activity was eliminated by 3% H_2O_2. Next, 6% normal goat serum containing primary antibodies was added for incubation overnight at 4°C. Color development was observed after 25 min of incubation with the appropriate secondary antibody at room temperature.

siRNA transfection

Cells were cultured in 6-well plates (for western blot analysis), 24-well plates (for immunofluorescence and lipid ROS detection) and 96-well plates (for cell viability assay). Control siRNA (no silencing) and Nrf2 siRNA were transfected into cells using a ribo*FECT*™ CP kit (RiboBio Co. Ltd., Guangzhou, China) according to the manufacturer's instructions. The siRNA target sequences are shown as below: si-Nrf2#1, CATTGATGTTTCTGATCTA; si-Nrf2#2, GAGGCAAGATATAGATCTT. All the analysis was performed at least 48h after transfection.

Establishment of rat models of cartilage damage

Four-week-old male SD rats were used in this study and allowed one week of routine feeding for adaptation. The rats' OA model was induced by destabilization of the medial meniscus (DMM) as previously described (Glasson et al., 2007; Sherwood et al., 2015). Cartilage degradation was evaluated histologically according to the Osteoarthritis Research Society International (OARSI) guidelines by two independent investigators. In addition, rats that died or appeared sick during experiments were excluded.

Animal experiment

42 rats were randomly divided into seven groups (n = 6 per group) after OA developed.

Group 1: sham surgery;

Group 2: DMM;

Group 3: DMM and intra-articular injection of DFO (1 mg/kg, twice a week);

Group 4: DMM and intra-articular injection of ASP (3 mg/kg, twice a week);

Group 5: erastin (1 mg/kg, one time) injection into the articular cavity;

Group 6: erastin (1 mg/kg, one time) and ASP (3 mg/kg, twice a week) injection into the articular cavity;

Group 7: erastin (1 mg/kg, one time) and DFO (1 mg/kg, twice a week) injection into the articular cavity.

The same treatment was performed on each rat. After 10 weeks, the rats were sacrificed, and the knees were harvested. We performed MRI for imaging examination and hematoxylin-eosin (H&E) and Masson staining for pathological examination.

Statistical Analysis

The data in this study are presented as the mean ± SD of at least three independent experiments. Differences between 2 groups were compared with Student's *t* test, and one-way ANOVA was used for comparisons of more than two groups. All quoted *P* values were 2-tailed, and values less than 0.05 were considered statistically significant.

Results

Ferroptosis is involved in OA cartilage degeneration.

Joint cartilage specimens from patients with stage III or IV (K-L score) OA who underwent total knee arthroplasty were used (Fig. 1A). OA groups had lower collagen II and higher MMP13 levels than the control group (Fig. 1B). We measured the expression of ferroptosis-related proteins between groups. The results showed that the knee cartilage from the OA groups had lower GPX4 and FTH1 levels than the control group knee cartilage (Fig. 1C, 1D, 1G). The OA groups presented lower GSH contents and higher MDA production under oxidative stress than the control group (Fig. 1E 1F).

ASP partially inhibits ferroptosis induced by erastin.

The number of cells and cell viability decreased after erastin treatment compared with the ASP treatment (Fig. 2A, 2B). LDH release decreased after pretreatment with ASP (Fig. 2C). Both ASP and Fer-1 partially reversed the erastin-induced reductions in GPX4, SLC7A11 and FTH1 (Fig. 2D- G). After pretreatment of chondrocytes with ASP, the lipid peroxidation induced by erastin was partially rescued (Fig. 2H).

ASP alleviates OA by inhibiting ferroptosis.

Chondrocytes were more active after treatment with ASP and DFO (an inhibitor of ferroptosis) than after treatment with IL-1β (pretreatment with IL-1β for 24 hours) (Fig. 3A). Both ASP and DFO suppressed the increase in ROS induced by IL-1β (Fig. 3b). ASP also reversed the decline in GPX4, FTH1, and SLC7A11 expression induced by IL-1β (Fig. 3C, 3D). We also used immunofluorescence to observe the expression level of GPX4, and the results were consistent with the western blot results (Fig. 3E, 3F). When chondrocytes were treated with IL-1β, MMP13 was increased and collagen II was decreased, but ASP reversed these effects (Fig. 3G, 3H, 3I).

ASP inhibits ferroptosis of OA chondrocytes via Nrf2-SLC7A11-GPX4 axis.

We used ASP to treat chondrocyte ferroptosis induced by erastin or IL-1β. As shown in Fig. 4A and 4B, NQO1 and HO-1 expression increased after treatment with ASP, while SLC7A11 expression changed with ASP treatment. We found that the protein levels of Nrf2 in the nucleus were increased in cells treated with ASP (Fig. 4C- 4E). Next, we silenced Nrf2 with a specific siRNA (Fig. 4F), the protective effect was lost (Fig. 4H), and the ROS of lipid was not changed. GPX4, SLC7A11, HO-1 and Nrf2 decreased due to knockdown, and the antioxidant capacity of cells decreased (Fig. 4I- K).

ASP or DFO alleviate the degeneration of cartilage in the imageology of rats

On MRI, the cartilage surface layer was destroyed, reduced and irregularly clustered in Group 2. In Group 3, cartilage damage was mild (Fig. 5A-C), which is consistent with the effect of extracorporeal treatment. The degree of cartilage destruction in Group 4 was lower than that in Group 2 (Fig. 5D). Group 5 also showed a certain degree of cartilage damage (Fig. 5E). Both Group 6 and Group 7 showed less cartilage destruction than Group 5 (Fig. 5F-G).

ASP or DFO alleviate the damage of cartilage in the pathology of rats

HE and Masson's trichrome staining showed severe cartilage destruction in Groups 2 and 5 (more severe in Group 2) (Fig. 6A 2, 5 and 6B 2, 5). However, the joint damage in Groups 3, 4, 6 and 7 was relatively mild (Fig. 6A 3, 4, 6, 7 and 6B 3, 4, 6, 7). In addition, GPX4 expression was lower in Group 2 and Group 5 (Fig. 6C 2, 5 and 6C 2, 5). However, the low GPX4 expression induced by MIA was alleviated by DFO and ASP treatment (Fig. 6C 3, 4). GPX4 expression in Groups 6 and 7 was higher than that in Group 5 (Fig. 6C).

Discussion

Chondrocytes are the only cells in articular cartilage and are responsible for maintaining functional tissue; thus, cartilage damage caused by chondrocyte programmed death plays an important role in the pathogenesis of osteoarthritis (Aigner et al., 2004; Kühn et al., 2004). Ferroptosis has been reported to influence the pathogenesis of OA (Bin et al., 2021; Reed et al., 2021; Simão and Cancela, 2021). With further research on ferroptosis in recent years, the main mechanism has gradually been uncovered, and one of the typical characteristics is excessive accumulation of lipid ROS (Yang and Stockwell, 2016). Ferroptosis can be triggered when the balance between lipid peroxidation and purging is disturbed. However, with the help of GSH, GPX4 converts toxic lipid hydroperoxide into a nontoxic lipid (Yang et al., 2014), and of course, FSP1 has the same effect (Doll et al., 2019). In our study, GPX4 was decreased in cartilage specimens from patients who underwent knee replacement (Fig. 1) and the OA rat models (Fig. 6C). Numerous studies have reported that ROS are the main cause of OA development (Aigner et al., 2004; Martin et al., 2004). ROS upregulates latent matrix-degrading enzyme production and inhibits matrix synthesis, effectively destroying cartilage homeostasis and inducing cell death (Haklar et al., 2002; Goldring and Berenbaum, 2004; Im et al., 2008). We found that erastin induced lipid ROS aggregation and ASP partially reversed this effect (Fig. 2H). Oxidative stress can lead to mitochondrial dysfunction, mitochondrial DNA damage, telomere instability, cell senescence and anabolic dysfunction (Finkel and Holbrook, 2000; Maneiro et al., 2005). Therefore, an increasing number of researchers have begun to focus on the effect of antioxidants on OA. Iron is thought to play an important role in the production of lipid peroxidation through the Fenton reaction and to act as a switch in ferroptosis (Wang et al., 2017).

Jing et al. showed that iron overload promotes chondrocyte breakdown (Jing et al., 2021). DFO, similar to Fer-1, is a known inhibitor of ferroptosis that prevents the occurrence of the Fenton reaction by chelating free Fe^{2+}. Interestingly, articular cartilage destruction was significantly alleviated in OA rats treated with DFO (Fig. 5C, 6A, 6B).

Next, in the search for anti-OA compounds, ASP caught our attention. Previous studies have shown that ASP has excellent antioxidant and antiapoptotic properties and induces chondrocyte proliferation (Xie et al., 2018; Xu et al., 2021). Although ASP has many protective effects on OA cartilage, no information is available regarding the effect of ASP on ferroptosis in OA (Zhuang et al., 2016; Zhuang et al., 2018). Although ferroptosis can be induced by erastin, this phenomenon is not consistent with the OA pathological developmental process. Thus, we used Il-1β to stimulate chondrocytes (from non-damaged regions) to simulate the OA environment (Kapoor et al., 2011). We found that Il-1β and erastin had similar ferroptosis induction effects (lipid ROS aggregation and GPX4, SLC7A11, and FTH1 decreases), which were reversed by ASP (Fig. 2, 3). ASP effectively reduces cartilage injury by erastin or DMM *in vivo* (Figs. 5, 6).

Keap1-Nrf2 signaling is considered one of the most critical endogenous antioxidant stress pathways and an important target of inflammation-related diseases (Mills et al., 2018; Lu et al., 2019). Convincingly, several compounds called Nrf2 activators have been shown to protect OA chondrocytes (Kim et al., 2020; Lv et al., 2021). Sun J et al. reported that inhibition of the Nrf2 pathway increased ferroptosis sensitivity (Sun et al., 2021). Previous studies have shown that Nrf2 protects cells from ferroptosis by promoting SLC7A11 expression (Procaccini et al., 2021; Tang et al., 2021), which is consistent with our results (Fig. 4). Nrf2 binds with Keap1 under non-stress conditions and is ubiquitinated and degraded in a Keap1-dependent manner (Sies et al., 2017). Interestingly, ASP can promote the dissociation of Keap1-Nrf2, the transfer of Nrf2 into the nucleus to exert an antioxidative effect, and SLC7A11 expression (Fig. 4A, 4B). Nrf2 was also slightly increased in response to IL-1β and Erastin, but we think that this increase is a stress effect of exogenous stimulation (Fig. 4A, B). To further investigate whether ASP functions through Nrf2, we knocked down Nrf2. The results showed that SLC7A11 expression was inhibited, lipid peroxidation product accumulation was increased, and the antiferroptotic ability of ASP was decreased (Fig. 4), suggesting that ASP can increase SLC7A11 expression by promoting the transfer of Nrf2 into the nucleus and subsequently protect chondrocytes from the reduction in SLC7A11 (Fig. 7).

In conclusion, our study suggests that ASP can increase SLC7A11 expression by promoting the transfer of Nrf2 into the nucleus to avoid chondrocyte ferroptosis. ASP may be a promising compound to alleviate OA in the future.

Declarations

Funding

This research was supported by the National Natural Science Foundation of China (82002321) to Liangliang Wang and the Natural Science Foundation of the Jiangsu for Youth (BK20180182) to Su Ni.

Competing interests

None declared.

Patient consent for publication

Not required.

Contributors

Yuji Wang contributed to the design and direction of the study. Guangrong Yin performed the main experiments. Shijie Jiang, Baojun Zhou and Ruixia Zhu contributed to the drafting of the article. Gongyin Zhao completed the acquisition or preparation of the clinical samples. Su Ni and Liangliang Wang contributed to the analysis and interpretation of the data. Nanwei Xu and Yuji Wang contributed to the critical revision and provided important intellectual feedback. All the authors read and approved the final manuscript.

References

1. Aigner T, Kim HA and Roach HI (2004) Apoptosis in osteoarthritis. Rheumatic diseases clinics of North America **30**:639–653, xi.
2. An S, Hu H, Li Y and Hu Y (2020) Pyroptosis Plays a Role in Osteoarthritis. Aging Dis **11**:1146–1157.
3. Bellezza I, Giambanco I, Minelli A and Donato R (2018) Nrf2-Keap1 signaling in oxidative and reductive stress. Biochimica et biophysica acta Molecular cell research **1865**:721–733.
4. Bin S, Xin L, Lin Z, Jinhua Z, Rui G and Xiang Z (2021) Targeting miR-10a-5p/IL-6R axis for reducing IL-6-induced cartilage cell ferroptosis. Experimental and molecular pathology **118**:104570.
5. Cao P, Sun J, Sullivan MA, Huang X, Wang H, Zhang Y, Wang N and Wang K (2018) Angelica sinensis polysaccharide protects against acetaminophen-induced acute liver injury and cell death by suppressing oxidative stress and hepatic apoptosis in vivo and in vitro. International journal of biological macromolecules **111**:1133–1139.
6. Dixon SJ, Lemberg KM, Lamprecht MR, Skouta R, Zaitsev EM, Gleason CE, Patel DN, Bauer AJ, Cantley AM, Yang WS, Morrison B, 3rd and Stockwell BR (2012) Ferroptosis: an iron-dependent form of nonapoptotic cell death. Cell **149**:1060–1072.
7. Dodson M, Castro-Portuguez R and Zhang DD (2019) NRF2 plays a critical role in mitigating lipid peroxidation and ferroptosis. Redox biology **23**:101107.
8. Doll S, Freitas FP, Shah R, Aldrovandi M, da Silva MC, Ingold I, Goya Grocin A, Xavier da Silva TN, Panzilius E, Scheel CH, Mourão A, Buday K, Sato M, Wanninger J, Vignane T, Mohana V, Rehberg M, Flatley A, Schepers A, Kurz A, White D, Sauer M, Sattler M, Tate EW, Schmitz W, Schulze A, O'Donnell

V, Proneth B, Popowicz GM, Pratt DA, Angeli JPF and Conrad M (2019) FSP1 is a glutathione-independent ferroptosis suppressor. Nature **575**:693–698.

9. Finkel T and Holbrook NJ (2000) Oxidants, oxidative stress and the biology of aging. Nature **408**:239–247.
10. Glasson SS, Blanchet TJ and Morris EA (2007) The surgical destabilization of the medial meniscus (DMM) model of osteoarthritis in the 129/SvEv mouse. Osteoarthritis Cartilage **15**:1061–1069.
11. Goldring MB and Berenbaum F (2004) The regulation of chondrocyte function by proinflammatory mediators: prostaglandins and nitric oxide. Clinical orthopaedics and related research:S37-46.
12. Gu P, Wusiman A, Wang S, Zhang Y, Liu Z, Hu Y, Liu J and Wang D (2019) Polyethylenimine-coated PLGA nanoparticles-encapsulated Angelica sinensis polysaccharide as an adjuvant to enhance immune responses. Carbohydrate polymers **223**:115128.
13. Haklar U, Yüksel M, Velioglu A, Turkmen M, Haklar G and Yalçin AS (2002) Oxygen radicals and nitric oxide levels in chondral or meniscal lesions or both. Clinical orthopaedics and related research:135–142.
14. Im HJ, Li X, Muddasani P, Kim GH, Davis F, Rangan J, Forsyth CB, Ellman M and Thonar EJ (2008) Basic fibroblast growth factor accelerates matrix degradation via a neuro-endocrine pathway in human adult articular chondrocytes. Journal of cellular physiology **215**:452–463.
15. Jiang S, Liu Y, Xu B, Zhang Y and Yang M (2020) Noncoding RNAs: New regulatory code in chondrocyte apoptosis and autophagy. Wiley Interdiscip Rev RNA **11**:e1584.
16. Jing X, Du T, Li T, Yang X, Wang G, Liu X, Jiang Z and Cui X (2021) The detrimental effect of iron on OA chondrocytes: Importance of pro-inflammatory cytokines induced iron influx and oxidative stress. Journal of cellular and molecular medicine **25**:5671–5680.
17. Kapoor M, Martel-Pelletier J, Lajeunesse D, Pelletier JP and Fahmi H (2011) Role of proinflammatory cytokines in the pathophysiology of osteoarthritis. Nature reviews Rheumatology **7**:33–42.
18. Kim EN, Lee HS and Jeong GS (2020) Cudratricusxanthone O Inhibits H(2)O(2)-Induced Cell Damage by Activating Nrf2/HO-1 Pathway in Human Chondrocytes. *Antioxidants (Basel, Switzerland)* **9**.
19. Kühn K, D'Lima DD, Hashimoto S and Lotz M (2004) Cell death in cartilage. Osteoarthritis Cartilage **12**:1–16.
20. Lu MC, Zhao J, Liu YT, Liu T, Tao MM, You QD and Jiang ZY (2019) CPUY192018, a potent inhibitor of the Keap1-Nrf2 protein-protein interaction, alleviates renal inflammation in mice by restricting oxidative stress and NF-κB activation. Redox biology **26**:101266.
21. Lv Z, Xu X, Sun Z, Yang YX, Guo H, Li J, Sun K, Wu R, Xu J, Jiang Q, Ikegawa S and Shi D (2021) TRPV1 alleviates osteoarthritis by inhibiting M1 macrophage polarization via Ca(2+)/CaMKII/Nrf2 signaling pathway. Cell death & disease **12**:504.
22. Maneiro E, López-Armada MJ, de Andres MC, Caramés B, Martín MA, Bonilla A, Del Hoyo P, Galdo F, Arenas J and Blanco FJ (2005) Effect of nitric oxide on mitochondrial respiratory activity of human articular chondrocytes. Annals of the rheumatic diseases **64**:388–395.

23. Martin JA, Brown TD, Heiner AD and Buckwalter JA (2004) Chondrocyte senescence, joint loading and osteoarthritis. Clinical orthopaedics and related research:S96-103.
24. Menegon S, Columbano A and Giordano S (2016) The Dual Roles of NRF2 in Cancer. Trends in molecular medicine **22**:578–593.
25. Mills EL, Ryan DG, Prag HA, Dikovskaya D, Menon D, Zaslona Z, Jedrychowski MP, Costa ASH, Higgins M, Hams E, Szpyt J, Runtsch MC, King MS, McGouran JF, Fischer R, Kessler BM, McGettrick AF, Hughes MM, Carroll RG, Booty LM, Knatko EV, Meakin PJ, Ashford MLJ, Modis LK, Brunori G, Sévin DC, Fallon PG, Caldwell ST, Kunji ERS, Chouchani ET, Frezza C, Dinkova-Kostova AT, Hartley RC, Murphy MP and O'Neill LA (2018) Itaconate is an anti-inflammatory metabolite that activates Nrf2 via alkylation of KEAP1. Nature **556**:113–117.
26. Moon EJ and Giaccia A (2015) Dual roles of NRF2 in tumor prevention and progression: possible implications in cancer treatment. Free radical biology & medicine **79**:292–299.
27. Procaccini C, Garavelli S, Carbone F, Di Silvestre D, La Rocca C, Greco D, Colamatteo A, Lepore MT, Russo C, De Rosa G, Faicchia D, Prattichizzo F, Grossi S, Campomenosi P, Buttari F, Mauri P, Uccelli A, Salvetti M, Brescia Morra V, Vella D, Galgani M, Mottola M, Zuccarelli B, Lanzillo R, Maniscalco GT, Centonze D, de Candia P and Matarese G (2021) Signals of pseudo-starvation unveil the amino acid transporter SLC7A11 as key determinant in the control of Treg cell proliferative potential. Immunity **54**:1543–1560.e1546.
28. Qiang Z, Dong H, Xia Y, Chai D, Hu R and Jiang H (2020) Nrf2 and STAT3 Alleviates Ferroptosis-Mediated IIR-ALI by Regulating SLC7A11. Oxidative medicine and cellular longevity **2020**:5146982.
29. Reed KSM, Ulici V, Kim C, Chubinskaya S, Loeser RF and Phanstiel DH (2021) Transcriptional response of human articular chondrocytes treated with fibronectin fragments: an in vitro model of the osteoarthritis phenotype. Osteoarthritis Cartilage **29**:235–247.
30. Riegger J and Brenner RE (2019) Evidence of necroptosis in osteoarthritic disease: investigation of blunt mechanical impact as possible trigger in regulated necrosis. Cell death & disease **10**:683.
31. Sharma L (2021) Osteoarthritis of the Knee. N Engl J Med **384**:51–59.
32. Sherwood J, Bertrand J, Nalesso G, Poulet B, Pitsillides A, Brandolini L, Karystinou A, De Bari C, Luyten FP, Pitzalis C, Pap T and Dell'Accio F (2015) A homeostatic function of CXCR2 signalling in articular cartilage. Annals of the rheumatic diseases **74**:2207–2215.
33. Sies H, Berndt C and Jones DP (2017) Oxidative Stress. Annual review of biochemistry **86**:715–748.
34. Simão M and Cancela ML (2021) Musculoskeletal complications associated with pathological iron toxicity and its molecular mechanisms. Biochemical Society transactions **49**:747–759.
35. Stockwell BR, Friedmann Angeli JP, Bayir H, Bush AI, Conrad M, Dixon SJ, Fulda S, Gascón S, Hatzios SK, Kagan VE, Noel K, Jiang X, Linkermann A, Murphy ME, Overholtzer M, Oyagi A, Pagnussat GC, Park J, Ran Q, Rosenfeld CS, Salnikow K, Tang D, Torti FM, Torti SV, Toyokuni S, Woerpel KA and Zhang DD (2017) Ferroptosis: A Regulated Cell Death Nexus Linking Metabolism, Redox Biology, and Disease. Cell **171**:273–285.

36. Sun J, Zhou C, Zhao Y, Zhang X, Chen W, Zhou Q, Hu B, Gao D, Raatz L, Wang Z, Nelson PJ, Jiang Y, Ren N, Bruns CJ and Zhou H (2021) Quiescin sulfhydryl oxidase 1 promotes sorafenib-induced ferroptosis in hepatocellular carcinoma by driving EGFR endosomal trafficking and inhibiting NRF2 activation. Redox biology **41**:101942.
37. Sun Y, Tang J, Gu X and Li D (2005) Water-soluble polysaccharides from Angelica sinensis (Oliv.) Diels: Preparation, characterization and bioactivity. International journal of biological macromolecules **36**:283–289.
38. Tang Z, Ju Y, Dai X, Ni N, Liu Y, Zhang D, Gao H, Sun H, Zhang J and Gu P (2021) HO-1-mediated ferroptosis as a target for protection against retinal pigment epithelium degeneration. Redox biology **43**:101971.
39. Toh WS, Lai RC, Hui JHP and Lim SK (2017) MSC exosome as a cell-free MSC therapy for cartilage regeneration: Implications for osteoarthritis treatment. Semin Cell Dev Biol **67**:56–64.
40. Tonelli C, Chio IIC and Tuveson DA (2018) Transcriptional Regulation by Nrf2. Antioxidants & redox signaling **29**:1727–1745.
41. Wang H, An P, Xie E, Wu Q, Fang X, Gao H, Zhang Z, Li Y, Wang X, Zhang J, Li G, Yang L, Liu W, Min J and Wang F (2017) Characterization of ferroptosis in murine models of hemochromatosis. Hepatology (Baltimore, Md) **66**:449–465.
42. Wang Q, Ding F, Zhu N, He P and Fang Y (2003) Determination of the compositions of polysaccharides from Chinese herbs by capillary zone electrophoresis with amperometric detection. Biomedical chromatography: BMC **17**:483–488.
43. Xie Y, Hou W, Song X, Yu Y, Huang J, Sun X, Kang R and Tang D (2016) Ferroptosis: process and function. Cell death and differentiation **23**:369–379.
44. Xie Y, Zhang H, Zhang Y, Wang C, Duan D and Wang Z (2018) Chinese Angelica Polysaccharide (CAP) Alleviates LPS-Induced Inflammation and Apoptosis by Down-Regulating COX-1 in PC12 Cells. Cellular physiology and biochemistry: international journal of experimental cellular physiology, biochemistry, and pharmacology **49**:1380–1388.
45. Xu C, Ni S, Zhuang C, Li C, Zhao G, Jiang S, Wang L, Zhu R, van Wijnen AJ and Wang Y (2021) Polysaccharide from Angelica sinensis attenuates SNP-induced apoptosis in osteoarthritis chondrocytes by inducing autophagy via the ERK1/2 pathway. Arthritis research & therapy **23**:47.
46. Yang WS, SriRamaratnam R, Welsch ME, Shimada K, Skouta R, Viswanathan VS, Cheah JH, Clemons PA, Shamji AF, Clish CB, Brown LM, Girotti AW, Cornish VW, Schreiber SL and Stockwell BR (2014) Regulation of ferroptotic cancer cell death by GPX4. Cell **156**:317–331.
47. Yang WS and Stockwell BR (2016) Ferroptosis: Death by Lipid Peroxidation. Trends in cell biology **26**:165–176.
48. Yao X, Sun K, Yu S, Luo J, Guo J, Lin J, Wang G, Guo Z, Ye Y and Guo F (2021) Chondrocyte ferroptosis contribute to the progression of osteoarthritis. J Orthop Translat **27**:33–43.
49. Zhuang C, Ni S, Yang ZC and Liu RP (2020) Oxidative Stress Induces Chondrocyte Apoptosis through Caspase-Dependent and Caspase-Independent Mitochondrial Pathways and the Antioxidant

Mechanism of Angelica Sinensis Polysaccharide. Oxidative medicine and cellular longevity **2020**:3240820.

50. Zhuang C, Wang Y, Zhang Y and Xu N (2018) Oxidative stress in osteoarthritis and antioxidant effect of polysaccharide from angelica sinensis. International journal of biological macromolecules **115**:281–286.
51. Zhuang C, Xu NW, Gao GM, Ni S, Miao KS, Li CK, Wang LM and Xie HG (2016) Polysaccharide from Angelica sinensis protects chondrocytes from H2O2-induced apoptosis through its antioxidant effects in vitro. International journal of biological macromolecules **87**:322–328.

Figures

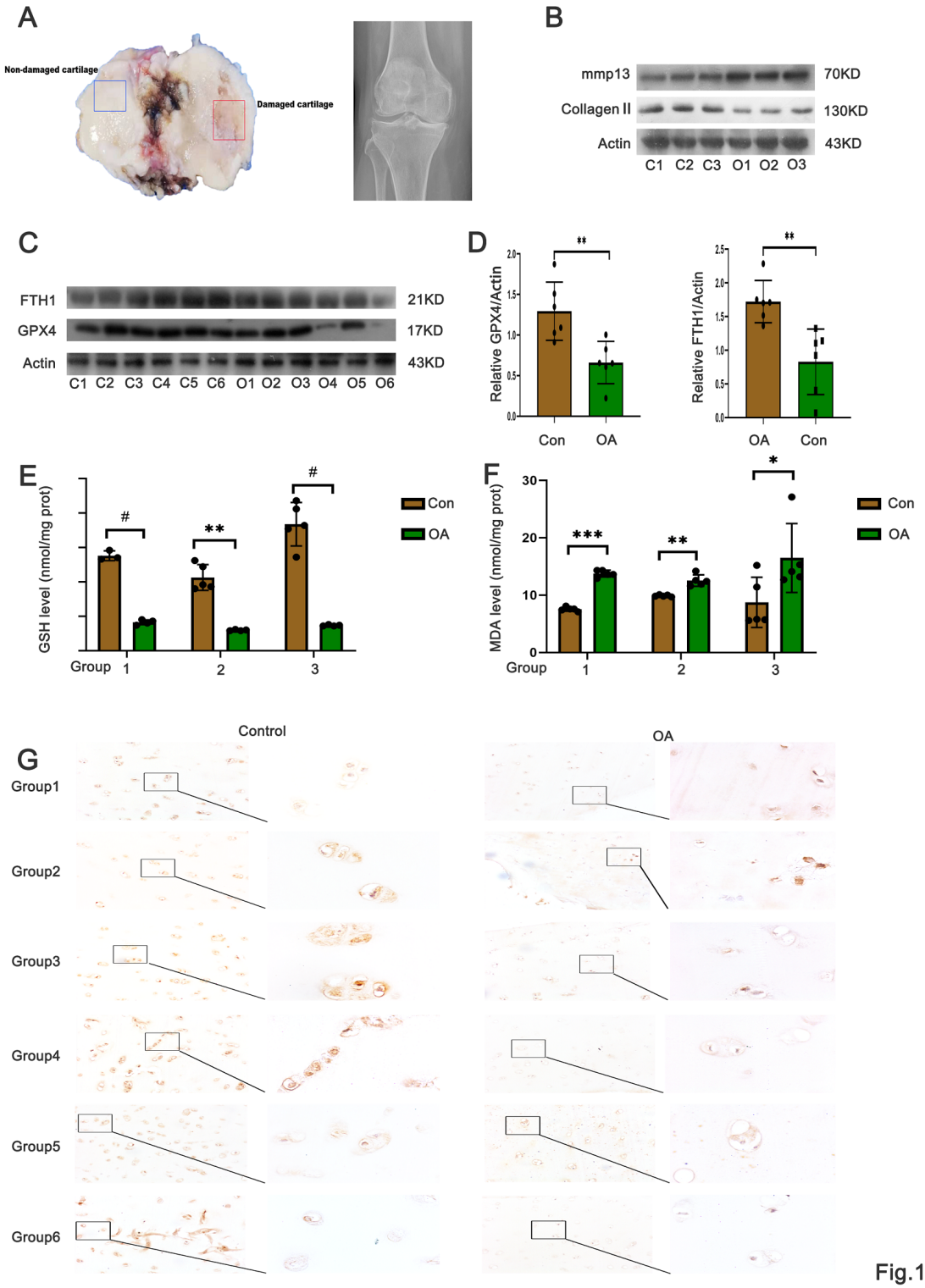

Fig.1

Figure 1

Ferroptosis involved in the OA cartilage degeneration. a: Representative image of articular cartilage of knee from patient underwent TKA showed damaged（OA group） and non-damaged regions（control group） and X-ray; **b:** 3 pairs of control and OA cartilages (each pair from the same joint) were ground with liquid nitrogen **c:** 6 pairs of control and OA cartilages were ground with liquid nitrogen. **d:** Quantification of the western blot result; **e-f:** The GSH and MDA levels in control and OA cartilages（ pairs 1-3 were

analyzed. **g:** Original magnification, ×100 (left), and ×400 (right). Each point represents an individual value (*p< 0.05, **p< 0.01, ***p< 0.001, #p< 0.0001).

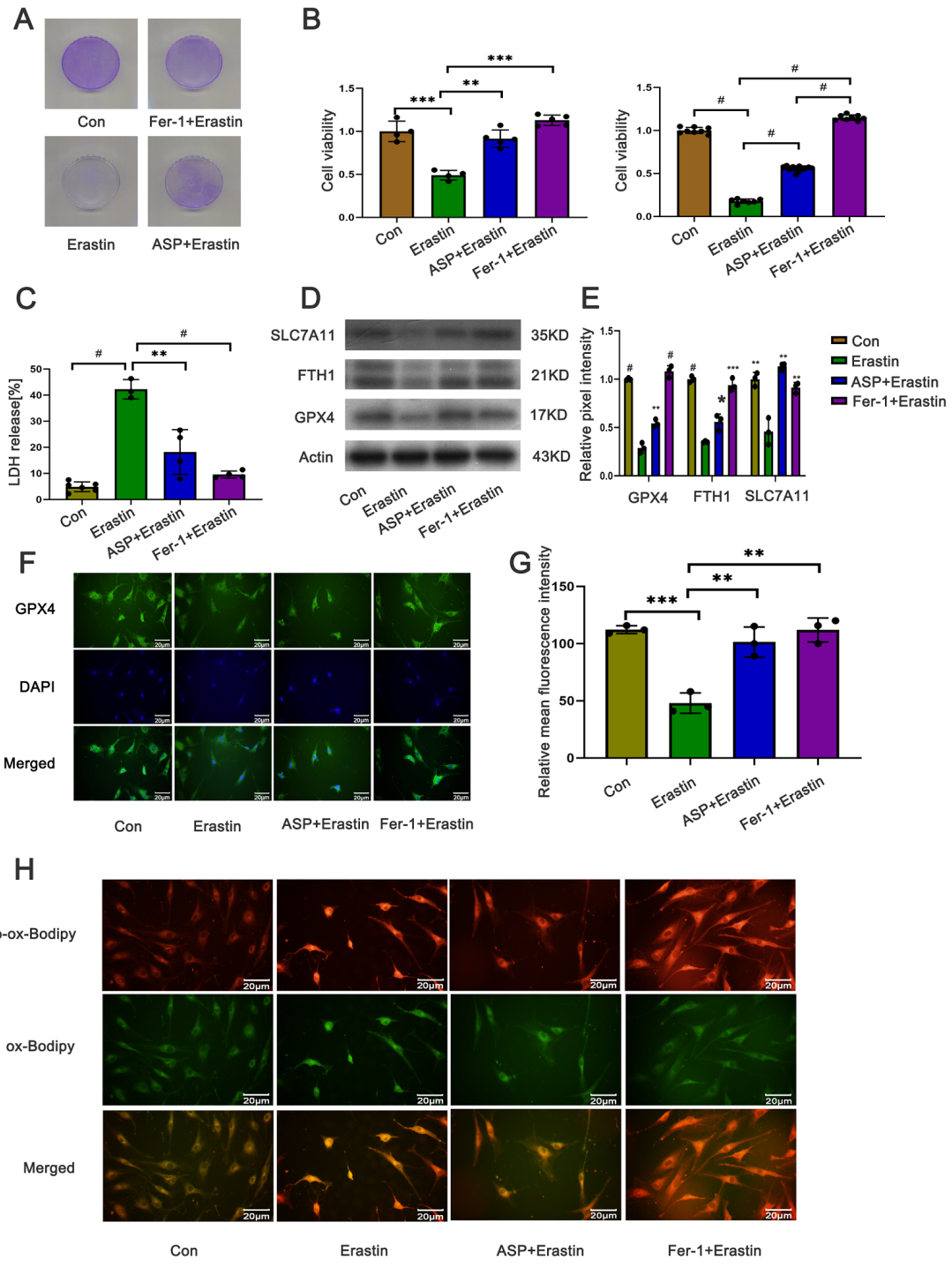

Fig.2

Figure 2

ASP partially inhibits chondrocyte ferroptosis induced by erastin. Chondrocytes were divided into four groups: control group (0.1% DMSO), erastin group, ASP+erastin group (ASP pretreated for 24 hours) and

Fer-1+erastin group (Fer-1 pretreated for 2 hours). **a:** The survival of chondrocytes was observed by crystal violet staining solution. **b:** Cell viability was analyzed with CCK-8. **c:** The lactate dehydrogenase released was analyzed with an LDH assay. **d-e:** The level of GPX4, FTH1 and SLC7A11 was measured by western blot. **f-g:** Original magnification, ×400. GPX4 immunostaining and quantification. Significantly increased green bright puncta showed the expression of GPX4. **h:** Original magnification, ×400. The accumulation of lipid peroxidation in cells was analyzed by BODIPY. Each point represents an individual value and no point means contrast (*p< 0.05, **p< 0.01, ***p< 0.001, #p< 0.0001).

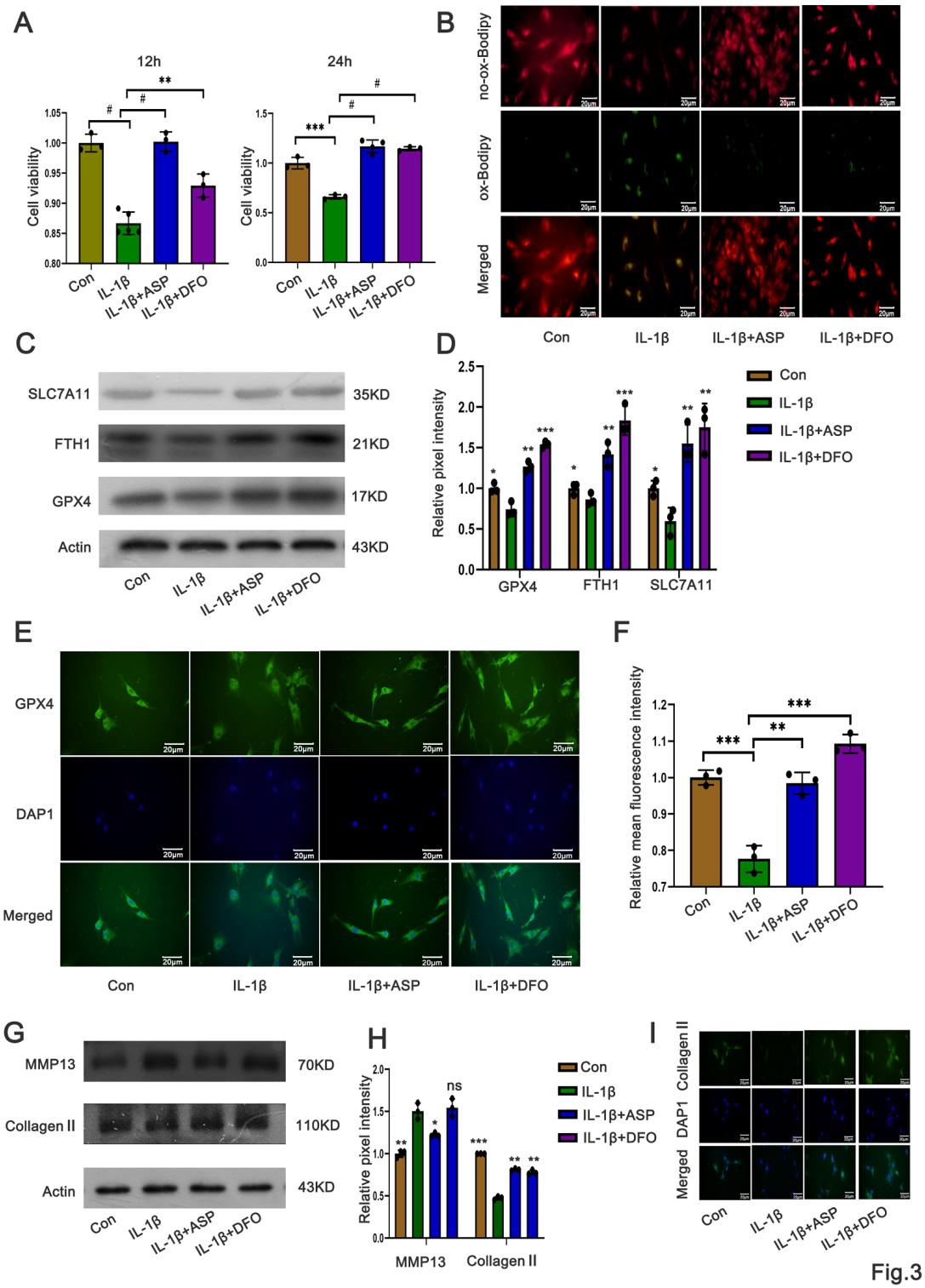

Fig.3

Figure 3

ASP can alleviate the injury of chondrocytes induced by IL-1β through ferroptosis. Chondrocytes were divided into four groups: control group (0.1% DMSO), IL-1β group, IL-1β+ASP group (IL-1β pretreated for 24 hours) and IL-1β+DFO group (IL-1β pretreated for 24 hours). **a:** Cell viability was analyzed with CCK-8 at 24 hours and 48 hours. **b:** Original magnification, ×400. The accumulation of lipid peroxidation in cells was analyzed by BODIPY. **c-d:** The level of GPX4, FTH1 and SLC7A11 was measured by western blot and quantification after 48 hours of treatment. **e-f:** Original magnification, ×400. Immunofluorescence and quantification. **g-h:** The level of MMP13 and collage and quantification after 48 hours of treatment. **i:** Original magnification, ×400. Immunofluorescence. Each point represents an individual value and no point means contrast (*p< 0.05, **p< 0.01, ***p< 0.001, #p< 0.0001).

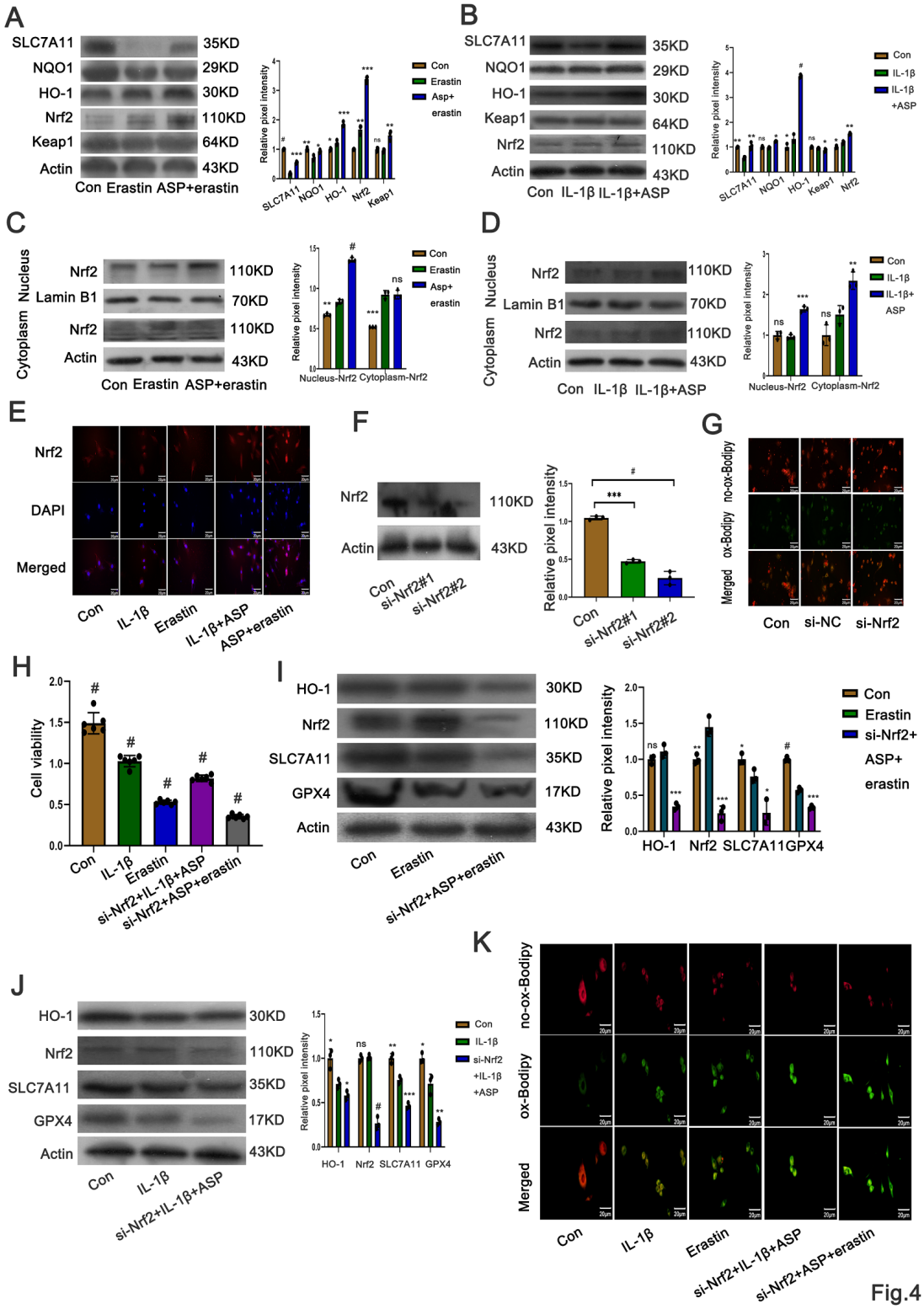

Figure 4

ASP inhibits ferroptosis through Nrf2. a-b: The level of Nrf2, Keap1, HO-1, NQO1 and SLC7A11 and quantification. **c-d:** Expression of Nrf2 in nucleus and cytoplasm and Quantification. **e:** Original magnification, ×400. Nrf2 immunostaining. Significantly increased red bright puncta showed the expression of Nrf2. **f:** The silencing efficiency of si-Nrf2 and quantification. **g:** Original magnification, ×400. The accumulation of lipid peroxidation in cells after Nrf2 silencing. **h:** Cell viability after si-Nrf2. **i-**

j: The level of GPX4, SLC7A11, Nrf2, and HO-1 and quantification. **k:** Original magnification, ×400. The accumulation of lipid peroxidation in cells after Nrf2 silencing. Each point represents an individual value and no point means contrast (**p< 0.01, ***p< 0.001, #p< 0.0001).

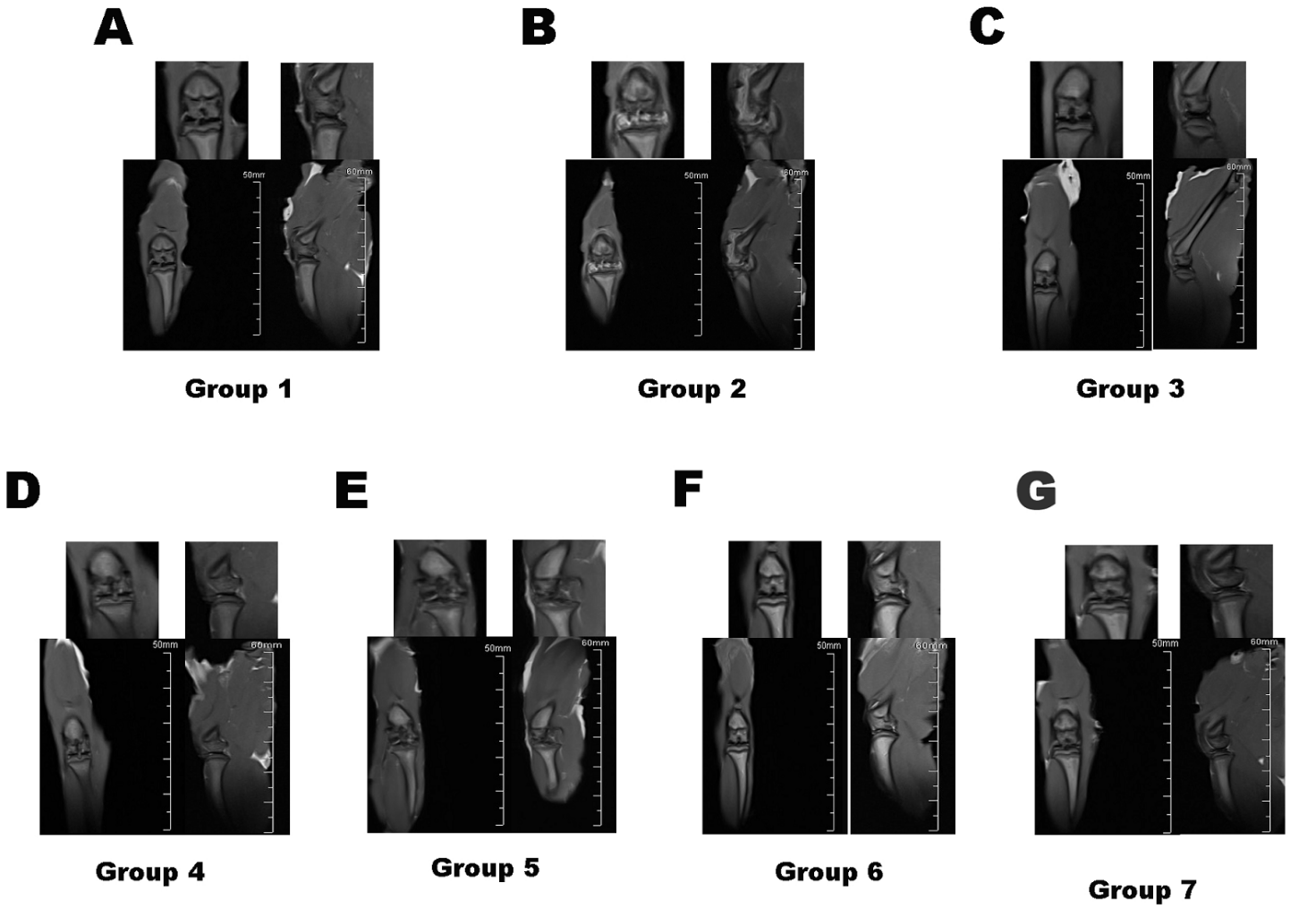

Figure 5

The changes of cartilage in rats were observed by imageology SD rats were divided into 7 groups: a: Control group, b: OA group c: OA+DFO group, d: OA+ASP group, e: Erastin group, f: erastin+ASP group, g: Erastin+DFO group.

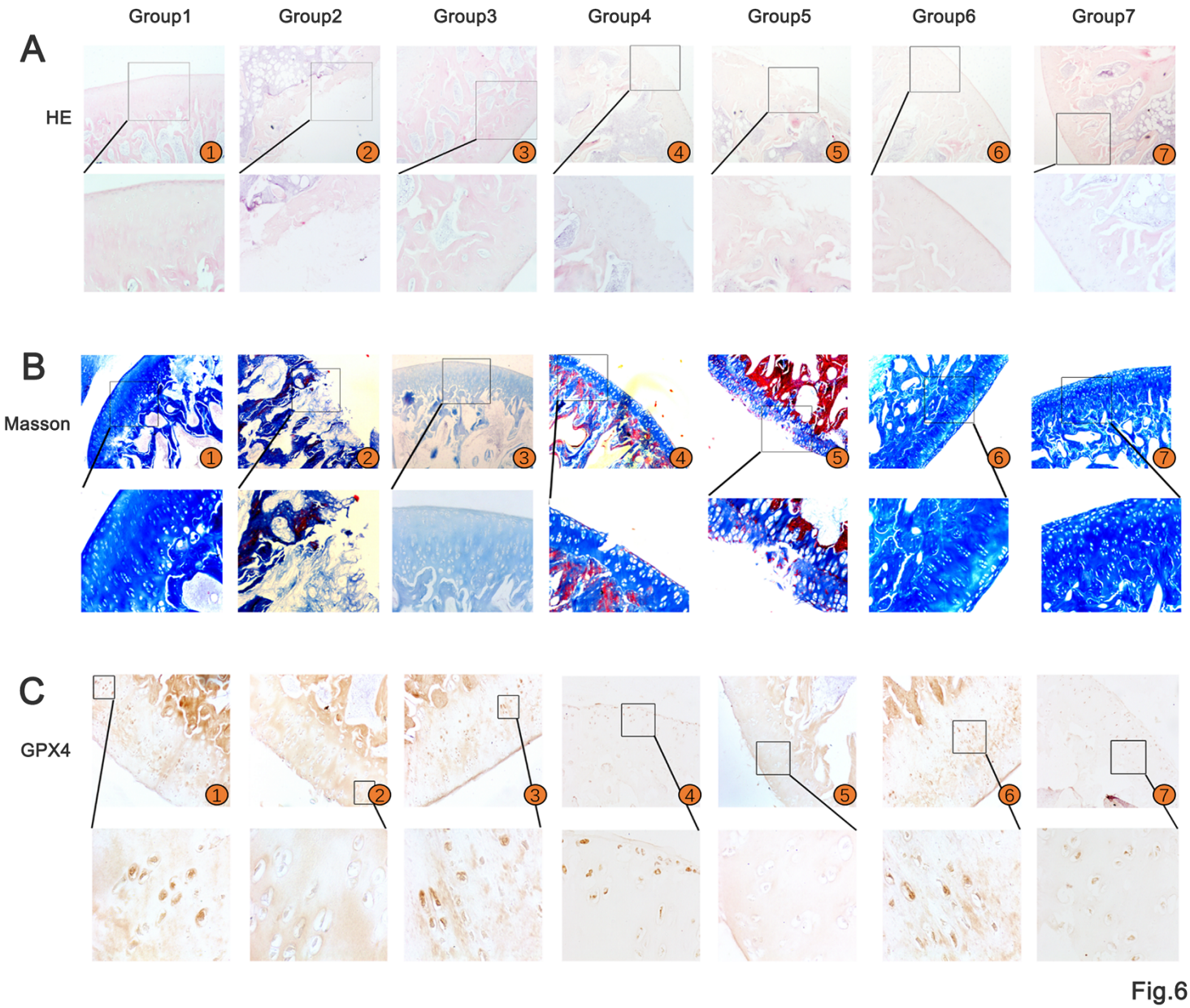

Figure 6

The changes of cartilage in rats were observed by pathology Original magnification, ×100 (upper), and ×400 (nether) Group 1-7 means Control group, OA group, OA+DFO group, OA+ASP group, Erastin group, Erastin+ASP group and Erastin+DFO group. **a:** The knee joint of rats was decalcified and stained with hematoxylin-eosin. **b:** Masson staining. **c:** Immunohistochemistry staining of GPX4.

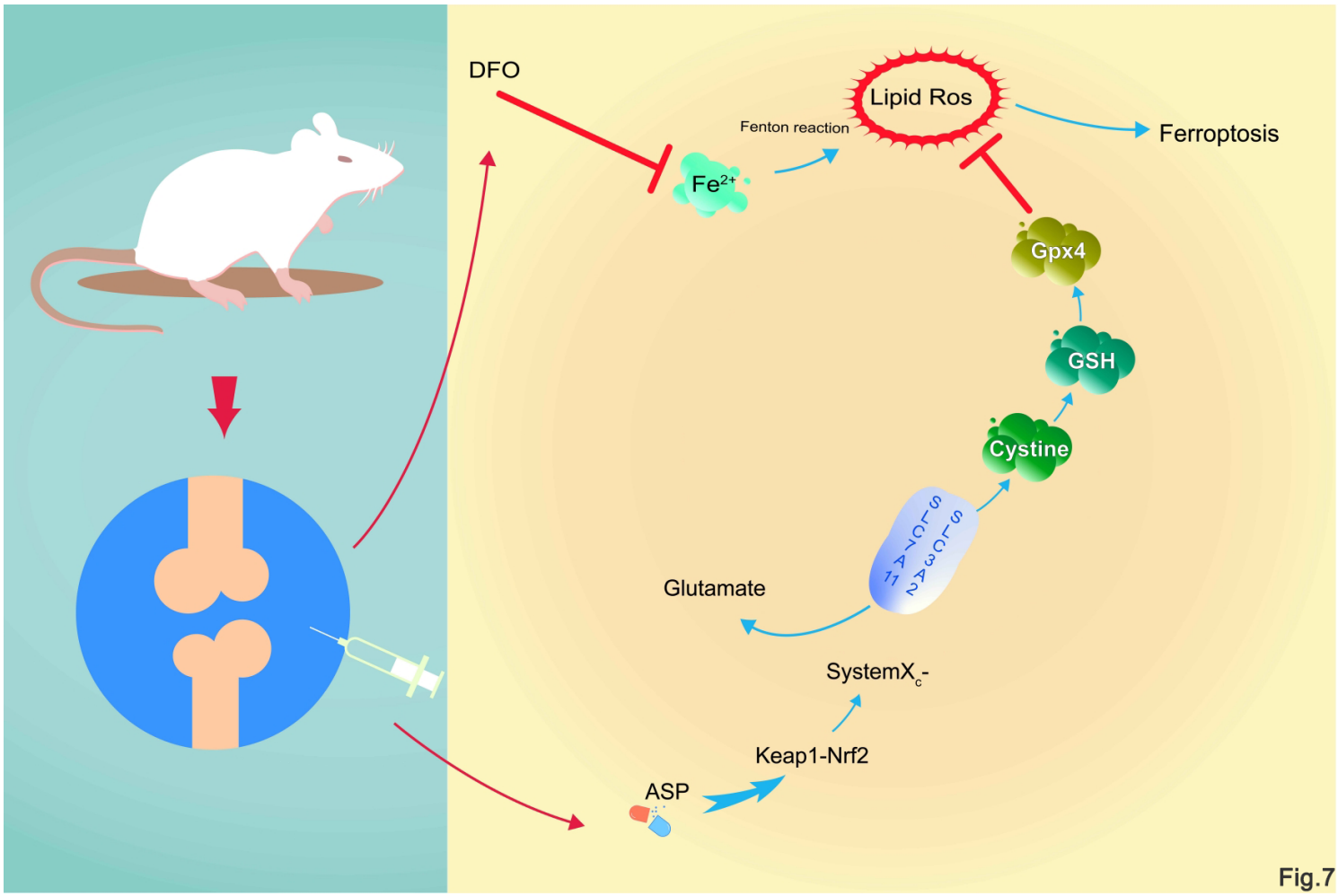

Figure 7

ASP alleviates OA by inhibiting ferroptosis via Nrf2-SLC7A11-GPX4 axis.

Supplementary Files

This is a list of supplementary files associated with this preprint. Click to download.

- Table.docx